INTEGRAL FLUXES, DAY-NIGHT, AND SPECTRUM RESULTS FROM SNO'S 391-DAY SALT PHASE

JÜRGEN WENDLAND
University of British Columbia
for the SNO Collaboration

The Sudbury Neutrino Observatory is a 1000 t heavy water Cherenkov detector observing neutrinos from the Sun and other astrophysical sources. Measurements of the integral solar neutrino fluxes of charged current, neutral current and elastic scattering events are reported for 391 days of live data from the salt phase of SNO operation. In this phase 2 t of salt were dissolved in the heavy water, which enhanced and differentiated the detection of neutral current events. Day-night asymmetries in these fluxes were also determined. The measured electron spectrum from the charged-current channel is compatible with the undistorted spectrum of the solar ^{8}B neutrino flux.

1. Solar Neutrinos

Solar neutrinos are produced in nuclear fusion processes in the center of the Sun, predominantly from the so-called *pp* cycle. These neutrinos have energies up to about 19 MeV. The flux of solar neutrinos arriving at Earth was measured prior to 2001 by a variety of experiments sensitive to various ranges in the neutrino energy spectrum. These experiments were exclusively or primarily sensitive to electron neutrinos and included radiochemical measurements using Cl or Ga and measurements of elastic scattering off electrons in light water Cherenkov detectors. The observed solar neutrino fluxes were two to three times smaller than those predicted by solar models[1,2,3].

This discrepancy may be explained by the oscillation of massive neutrinos giving rise to flavor change in neutrinos. The formalism for this process was introduced by Maki, Nakagawa, Sakata, and Pontecorvo (MNSP)[4,5] and was expanded to include matter-enhanced oscillations in the Earth or the Sun by Mikheyev, Smirnov, and Wolfenstein (MSW)[6,7]. In a two neutrino flavor model the mixing of the two neutrino flavor eigenstates ν_e and ν_μ is described by the mixing angle θ with respect to the neutrino mass eigenstates ν_1 and ν_2 and the difference of the squared neutrino masses

$\Delta m^2 = m_2^2 - m_1^2$. The survival probability for an electron neutrino in vacuum is then $P(\nu_e \to \nu_e) = 1 - \sin^2 2\theta \sin^2(1.27\Delta m^2\, L/E)$, where L is the distance traveled in km and E the neutrino energy in MeV. In matter the mixing angle depends on the electron density N_e of the medium, $\tan^2\theta_M = \tan\theta/(1 - 2\sqrt{2}EG_F N_e/(\Delta m^2 \cos 2\theta))$. The hypothesis of solar neutrino flavor transformation was first directly verified with measurements by the Sudbury Neutrino Observatory (SNO), which included a measurement of the total flux of solar ^{8}B neutrinos via the neutral current reaction in pure heavy water[9,10,11,12].

2. The Sudbury Neutrino Observatory

SNO is a 1000 t pure heavy water Cherenkov detector located 2039 m ($\sim$ 6000 mwe) underground in the Inco Creighton Mine near Sudbury, Ontario, Canada[8]. The heavy water is contained in a 12 m diameter acrylic vessel which is surrounded by $\sim$7,000 t of light water. 9,456 photomultiplier tubes (PMTs) that provide a photocathode coverage of 54 % are used to observe neutrino induced Cherenkov events.

SNO detects neutrinos via elastic scattering from electrons (ES, $\nu_x + e^- \to \nu_x + e^-$), and via the charged current (CC, $\nu_e + d \to p + p + e^-$) and neutral current reactions (NC, $\nu_x + d \to n + p + \nu_x$) on the deuteron. The ES reaction is sensitive to all neutrino flavors, but the electron neutrino sensitivity is higher than the others by a factor of about 6.5. The CC reaction is exclusively sensitive to electron neutrinos, whereas the NC reaction is equally sensitive to all active neutrino flavors.

The detection of the neutron is critical for the identification of the NC reaction. During SNO's first of three phases of operation the neutron was detected in pure heavy water via photon emission induced by neutron capture on deuterons. In the second phase, the addition of 2 t of salt to the heavy water enhanced the neutron detection via capture on chlorine and enabled a statistical separation of the NC and CC events through measurement of the isotropy of events on the phototubes. For the ongoing third phase, a discrete array of 40 ^{3}He-filled proportional counters for individual neutron detection was deployed in the heavy water.

3. The SNO Salt Phase

Neutron capture on ^{35}Cl in the salt increases the neutron detection efficiency by about a factor three compared to pure heavy water. In the subsequent de-excitation of ^{36}Cl a cascade of photons with a total energy

of 8.6 MeV is released. In comparison to the pure heavy water phase where neutron capture resulted in a 6.25 MeV photon, the energy profile of the radiative capture photopeak is thus moved further above the analysis threshold. In addition the multi-photon signature of neutron capture on chlorine is more isotropic than the single-ring Cherenkov events from the CC and ES interactions. Event light isotropy thus provides an additional means of distinguishing these event classes.

To obtain the rate of the CC, ES, and NC reactions and the energy spectrum of the CC events an extended maximum likelihood fit was applied to 4722 neutrino candidate events from the 391-day salt phase data set[13]. Probability density functions for each of the reactions and for an external neutron background were generated by a detailed Monte Carlo simulation of the detector in terms of the following parameters: event energy (T_{eff}), event direction ($\cos\theta_\odot$), volume weighted radius ($\rho = (R/R_{AV})^3$, $R_{AV} = 600.5\,\mathrm{cm}$), and event isotropy ($\beta_{14}$). The inclusion of event isotropy allowed a fit to the energy spectrum of the CC events that was not constrained to the spectral shape of solar ^{8}B neutrinos. Systematic uncertainties on the detector response were measured by comparing data from the Monte Carlo simulation with data from calibration sources. By propagating these uncertainties through the signal extraction process their effects on the fit parameters were determined.

The fluxes of the CC, ES, and NC channels obtained in this fit are respectively in units of $10^6\,\mathrm{cm}^{-2}s^{-1}$: $\phi_{\mathrm{CC}} = 1.68 \pm 0.06\,(\mathrm{stat})^{+0.08}_{-0.09}\,(\mathrm{sys})$, $\phi_{\mathrm{ES}} = 2.35 \pm 0.22\,(\mathrm{stat}) \pm 0.15\,(\mathrm{sys})$, and $\phi_{\mathrm{NC}} = 4.94 \pm 0.21\,(\mathrm{stat})^{+0.38}_{-0.34}\,(\mathrm{sys})$. These fluxes are the equivalent fluxes of ^{8}B electron neutrinos above an energy threshold of zero assuming an undistorted spectral shape. The main sources of systematic uncertainties are the isotropy measurement, the energy scale and bias, the event reconstruction biases, the neutron detection efficiency (NC flux only) and the angular resolution (ES flux only). The ratio of the CC and NC flux is $\phi_{\mathrm{CC}}/\phi_{\mathrm{NC}} = 0.340 \pm 0.023(\mathrm{stat})^{+0.029}_{-0.031}(\mathrm{sys})$, providing clear evidence that solar electron neutrinos change flavor in transit to the Earth.

The energy spectrum of the solar CC flux is shown in the left hand panel of Fig. 1. The expected shapes for an undistorted ^{8}B solar neutrino flux and for the best fit MSW model, see below, are also shown.

For certain ranges of mixing parameters the MSW effect predicts a regeneration of solar electron neutrinos when they pass through the Earth. The regeneration could be measurable as an asymmetry $A_{DN} = 2\,(\phi_N - \phi_D)/(\phi_N + \phi_D)$ of the solar neutrino flux ϕ_N measured at SNO

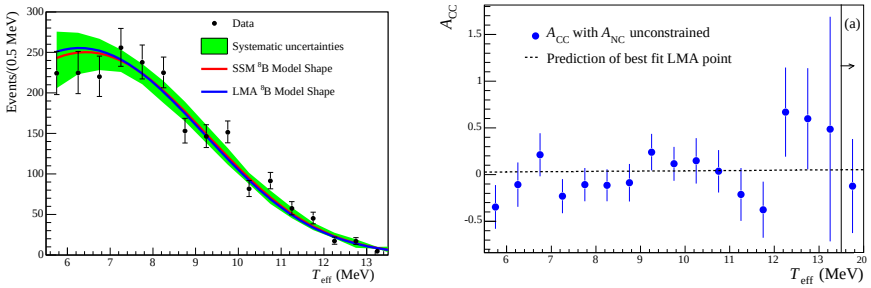

Figure 1. Left: The energy spectrum of the solar neutrino CC flux. The error bars are the statistical uncertainties. The band on the undistorted ^{8}B model shape represent the detector systematic uncertainties. Note that the data points are statistically and systematically correlated. Right: The day-night asymmetry of the charged current solar neutrino flux as a function of energy. The errors bars show the statistical uncertainties, and the horizontal line shows the expectation for the best fit MSW parameters.

during the night and the flux measured during the day ϕ_D. The energy-unconstrained analysis described above was carried out separately for the day and night neutrino candidate events. The resulting asymmetries in the CC, NC, and ES fluxes are $A_{\rm CC} = -0.056 \pm 0.074({\rm stat}) \pm 0.053({\rm sys})$, $A_{\rm NC} = 0.042 \pm 0.086({\rm stat}) \pm 0.072({\rm sys})$, and $A_{\rm ES} = 0.146 \pm 0.198({\rm stat}) \pm 0.033({\rm sys})$, respectively, where the systematics largely cancel in the asymmetry ratio. The day-night asymmetry of the CC flux as a function of electron energy is shown in the right hand panel of Fig. 1. Within the uncertainties the asymmetry is compatible with zero and with the best fit MSW solution, discussed in the following.

In an MSW two-parameter fit the presented results were combined with the global solar neutrino data set from SNO's pure heavy water phase, the Cl[14] and Ga[15,16] experiments and with the Super-Kamiokande zenith spectra[17]. Assuming CPT invariance the rates and spectra of the KamLAND experiment were also included to further restrict the allowed parameter space. The result of this neutrino oscillation analysis is shown in Fig. 2. The best fit point, $\Delta m^2 = 8.0^{+0.6}_{-0.4} \cdot 10^{-5}\,{\rm eV}^2$ and $\theta = 33.9 \pm^{+2.4}_{-2.2}$ degrees, lies in the large mixing angle (LMA) region. In this fit the SNO data provide strong constraint of the mixing angle.

4. Summary

The SNO collaboration has completed the salt phase data acquisition. Integral fluxes of the CC, NC, and ES reaction rates were extracted from

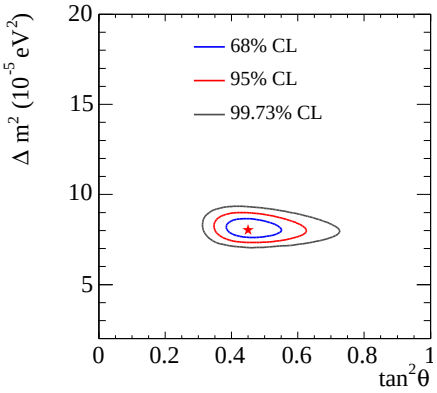

Figure 2. Neutrino oscillation contours in MSW parameter space for two flavor mixing. The best fit point is indicated by the star.

the full salt data set. The electron energy spectrum of the solar electron neutrino flux was observed with the charged current reaction and the day-night solar neutrino flux asymmetries were measured. The spectrum and the day-night asymmetries are consistent with the no-oscillation hypothesis and with the prediction by the best fit MSW LMA solution, which was determined in an MSW fit to global solar plus KamLAND data.

References

1. J. N. Bahcall and M. H. Pinsonneault, Phys. Rev. Lett. **92**, 121301 (2004).
2. J. N. Bahcall, A. M. Serenelli and S. Basu, Astrophys. J. **621**, L85 (2005).
3. S. Turck-Chieze *et al.*, Phys. Rev. Lett. **93**, 211102 (2004).
4. Z. Maki, M. Nakagawa and S. Sakata, Prog. Theor. Phys. **28**, 870 (1962).
5. V. N. Gribov and B. Pontecorvo, Phys. Lett. B **28**, 493 (1969).
6. S. P. Mikheev and A. Y. Smirnov, Sov. J. Nucl. Phys. **42**, 913 (1985).
7. L. Wolfenstein, Phys. Rev. D **17**, 2369 (1978).
8. J. Boger *et al.* [SNO], Nucl. Instrum. Meth. A **449**, 172 (2000).
9. Q. R. Ahmad *et al.* [SNO], Phys. Rev. Lett. **87**, 071301 (2001).
10. Q. R. Ahmad *et al.* [SNO], Phys. Rev. Lett. **89**, 011301 (2002).
11. Q. R. Ahmad *et al.* [SNO], Phys. Rev. Lett. **89**, 011302 (2002).
12. S. N. Ahmed *et al.* [SNO], Phys. Rev. Lett. **92**, 181301 (2004).
13. B. Aharmim *et al.* [SNO], arXiv:nucl-ex/0502021.
14. B. T. Cleveland *et al.*, Astrophys. J. **496**, 505 (1998).
15. V. N. Gavrin [SAGE], Nucl. Phys. Proc. Suppl. **138**, 87 (2005).
16. M. Altmann *et al.* [GNO], Phys. Lett. B **490**, 16 (2000).
17. S. Fukuda *et al.* [Super-Kamiokande], Phys. Lett. B **539**, 179 (2002).